Use of a narrow-gap prewell for the optical study of charge buildup and the Fermi-energy edge singularity in a double-barrier resonant-tunneling structure

T. A. Fisher
Department of Physics, University of Sheffield, Sheffield S3 7RH, United Kingdom
and Department of Physics, University of Wollongong, Wollongong, New South Wales 2500, Australia

P. D. Buckle
Department of Physics, University of Sheffield, Sheffield S3 7RH, United Kingdom

P. E. Simmonds
Department of Physics, University of Wollongong, Wollongong, New South Wales 2500, Australia

R. J. Teissier* and M. S. Skolnick
Department of Physics, University of Sheffield, Sheffield S3 7RH, United Kingdom

C. R. H. White
Department of Physics, University of Nottingham, Nottingham NG7 2RD, United Kingdom

D. M. Whittaker
Department of Physics, University of Sheffield, Sheffield S3 7RH, United Kingdom

L. Eaves
Department of Physics, University of Nottingham, Nottingham NG7 2RD, United Kingdom

B. Usher and P. C. Kemeny
Telecom Research Laboratories, Clayton, Victoria 3168, Australia

R. Grey, G. Hill, and M. A. Pate
Department of Electronic and Electrical Engineering, University of Sheffield, Sheffield S1 3JD, United Kingdom
(Received 4 April 1994; revised manuscript received 20 June 1994)

A strained $In_yGa_{1-y}As$ layer is incorporated adjacent to the emitter barrier of an $Al_xGa_{1-x}As/GaAs/Al_xGa_{1-x}As$ double-barrier resonant-tunneling structure (DBRTS), so that it forms a prewell for the electrons that accumulate prior to tunneling into the GaAs quantum well (QW). Observation of photoluminescence (PL) and photoluminescence excitation (PLE) from the prewell then enables a direct optical determination of the charging behavior in the emitter-accumulation region to be achieved. We show in addition that an optical probe of the prewell can, by consideration of the electrostatics, provide a reliable determination of the charge distribution in the whole DBRTS at the peak of the tunneling resonance. These results are shown to be in agreement with separate determinations of the charge in the GaAs QW by direct PL measurements, and of the charge in the emitter-accumulation layer from magnetotransport studies. The electron density in the prewell can be varied continuously over a wide range, from 0 to 9×10^{11} cm^{-2}. The second subband is populated at high applied bias, with the density varying from 0 to 1×10^{11} cm^{-2}. This structure is then very well suited to the study of the many-body nature of the excitonic enhancement near the absorption threshold, over a much wider range of electron densities than previously studied on an individual sample. Utilizing temperature-dependent PLE measurements, we have monitored the variation from an atomic exciton in $n=1$, to a Fermi-energy edge singularity (FEES) in $n=1$, through to a FEES in $n=2$, in the same sample.

I. INTRODUCTION

Double-barrier resonant-tunneling structures (DBRTS's) were first discussed in 1973–1974.[1] When bias is applied to a DBRTS, with low-contact doping near the barriers, a two-dimensional electron gas is formed in the emitter-accumulation region.[2–5] In such structures, with relatively thin barriers of the same width, a sharply peaked feature in the current-voltage (I-V) characteristics is observed on resonance. With incorporation of asymmetric barriers, where the collector barrier is wider than the emitter barrier, charge accumulation in the quantum well between the barriers is enhanced.[2–9] This is shown by an extended resonance in the I-V characteristics, and in many cases by the occurrence of intrinsic bistability.[2–5,8]

0163-1829/94/50(24)/18469(10)/$06.00

Originally DBRTS's were investigated principally by transport techniques. Photoluminescence from the quantum-well (QW) region of a DBRTS was first observed by Young *et al.*[10] It was subsequently shown by Skolnick *et al.*[8] that band-filling effects on the photoluminescence (PL) linewidth, as a function of applied bias V_B, can provide a direct measure of charge buildup in the QW part of the DBRTS on resonance. Photoluminescence excitation (PLE) studies of charge-density variations in DBRTS's have also been performed.[9,11,12] Until recently the only method available to directly study the two-dimensional (2D) electron gas in the emitter-accumulation region was magnetotransport where study of magneto-oscillations in the current or capacitance as the Fermi level moves between Landau levels allows determination of the electron density.[5,4,2]

In the structure studied here a shallow $In_yGa_{1-y}As$ layer has been incorporated adjacent to the emitter barrier.[13] The $(In_yGa_{1-y})As$ layer forms a prewell, into which electrons accumulate into 2D states, prior to tunneling through the double-barrier region. Holes, directly photocreated in the prewell, are inhibited from being swept into the contact region by the prewell barrier, thus allowing photoluminescence to be observed from the emitter-accumulation region. As a result we now have an all optical means to study directly the buildup of charge in the emitter-accumulation region of the DBRTS under operation. Furthermore, the PL from the $In_yGa_{1-y}As$ prewell occurs at lower energies than the band gap of the GaAs contact regions, and is only attenuated very slightly by absorption in the GaAs.

In this paper we present low-temperature PL and PLE results from the prewell of a DBRTS with asymmetric barriers. We show, by consideration of the electrostatics involved, that an optical probe of the emitter-accumulation region can be used to understand the charge distribution across the whole DBRTS as a function of applied bias. These results agree well with separate PL measurements from the GaAs QW, and with the trends of a magnetotransport determination of the electron density in the prewell emitter-accumulation region. In this asymmetric DBRTS the increase in charge density of the prewell with bias is interrupted while the structure is on resonance; the prewell density remains constant while the GaAs QW is charging up.

The charge density in the prewell (n_p) varies from $n_p=0$ to $\simeq 9\times 10^{11}$ cm^{-2}, with a significant population in the second subband (up to $n_{p,2}\simeq 1\times 10^{11}$ cm^{-2}) at higher densities. Optical techniques are a very sensitive way of detecting the occupation of the second $n=2$ subband, since PL is observed as soon as the Fermi energy ε_F, measured relative to the $n=1$ subband edge, is equal to the subband-edge spacing E_2-E_1. On the other hand, with magnetotransport techniques $n=2$ population is only observed when $n_{p,2}$ is greater than $\sim 0.8\times 10^{11}$ cm^{-2}. Simple self-consistent calculations of the electronic structure of the prewell with n_p were also carried out. The calculated changes with n_p in the energies and oscillator strengths of intersubband optical transistors were found to be in good agreement with the trends observed in the experiments.

The wide controllable variation in charge density in the prewell also means that this structure is ideal for studying the Fermi-energy edge singularity (FEES) (Refs. 14–22) over a greater range of carrier densities than previously studied on an individual sample. Previous measurements as a function of density have in general, either studied the FEES in $n=1$ (Refs. 16 and 17) or in $n=2$.[18,22] In PLE (or optical absorption) the FEES appears as an excitonic enhancement at the threshold of transitions into unoccupied states above the Fermi level E_F. The FEES arises due to correlation between the photoexcited hole and the high-density Fermi sea of the electrons.[19] The characteristic spectral behavior is a decrease in oscillator strength and broadening of the excitonlike enhancement up to temperatures of 50 K. This is a result of the Fermi surface broadening and consequent weakening of the electron-hole interaction.[14–17] In Refs. 22 and 18 it was found that the existence of a FEES depended only on the carrier density of the subband with which it is associated. Using temperature-dependent PLE of the prewell transitions we have followed the spectral variation with n_p from an atomic exciton in $n=1$, to a FEES in $n=1$, through to a FEES in $n=2$.

The paper is organized in the following way. In the next section details of the DBRTS and the experiments are given. The charging characteristics of the DBRTS's are discussed in Sec. III. In Secs. III A, III B, and III C the current-voltage characteristics and the PL and PLE results from the prewell are presented. The optical results are then used to provide a measure of the prewell electron accumulation in Sec. III D. In Sec. III E experimental results are compared with the self-consistent calculations. Section III F correlates the GaAs QW charge deduced from the prewell studies with that from direct PL measurements of the GaAs QW. In Sec. IV Fermi-energy edge singularity studies from the prewell of the DBRTS are presented. The conclusion is given in Sec. V.

II. EXPERIMENT

The experiments were carried out on an $Al_xGa_{1-x}As/GaAs/Al_xGa_{1-x}As$ DBRTS containing a shallow $In_yGa_{1-y}As$ prewell layer. Details of the structure are given in Table I. The DBRTS consists of a 60-Å

TABLE I. Sample characteristics.

Composition	Structure *A*
n^+ GaAs contact	1 μm, 1×10^{18} cm^{-3}
	500 Å, 1×10^{16} cm^{-3}
GaAs	50 Å
$Al_xGa_{1-x}As$	$x=0.33$, 120 Å
GaAs	60 Å
$Al_xGa_{1-x}As$	$x=0.33$, 80 Å
$In_yGa_{1-y}As$	$y=0.05$, 250 Å
GaAs	50 Å
n^+ GaAs contact	500 Å, 1×10^{16} cm^{-3}
	1 μm, 1×10^{18} cm^{-3}
	GaAs substrate

GaAs QW and asymmetric $Al_xGa_{1-x}As$ ($x=0.33$) barriers of width 80 and 120 Å. The $In_yGa_{1-y}As$ ($y=0.05$) layer of width 250 Å is grown adjacent to the narrower barrier, and is on the substrate side of the barriers. The width of the $In_{0.05}Ga_{0.95}As$ layer is 250 Å, well below the critical thickness for strain relief.[23] The contact-layer doping is graded and has low doping close to the barriers; together with the incorporation of spacer layers, this facilitates 2D electron gas accumulation in the emitter-accumulation region over the whole bias range of interest.[2–4] Except for the inclusion of the $In_yGa_{1-y}As$ prewell layer, structure *A* is very similar to the asymmetric structure reported in Refs. 3–5 and 8 and has similar optical and electrical properties. Mesas of 100–300 μm diameter were employed, with annular contacts to permit optical access.

Photoluminescence and photoluminescence excitation measurements at $T=4$ K were excited with a tunable Ti:sapphire laser, or He-Ne laser for PL only, dispersed with a 0.75-m double grating spectrometer and detected by a liquid-nitrogen-cooled Ge photodiode or a thermoelectrically cooled GaAs photomultiplier. The excitation intensity of 5 W/cm^2 did not significantly perturb the *I-V* characteristics. Magnetotransport measurements were carried out with an 11.4-T vertical bore superconducting magnet. The mesa used for the magnetotransport measurements was smaller (100 μm) than the one used for the principal optical measurements (200 μm).

III. CHARGE DISTRIBUTION BEHAVIOR

A. Electrical measurements

In the forward bias direction (top contact positive) the current versus voltage (*I-V*) characteristics of the structure display two resonances with peaks in the current at biases of $V_B=0.66$ and 1.48 V. The positions of the resonances are very similar, as expected, to the similarly designed asymmetric structure (except for the prewell) of Refs. 2–4 and 8; as expected the prewell causes very little perturbation of the *I-V* characteristics. In the present work the bias region near the first resonance, up to 1.2 V, is studied in detail. *I-V* characteristics taken with the illumination conditions employed for the optical measurements, and sweeping V_B in the forward direction, are shown in Fig. 1(a).

The calculated potential profile of the conduction and valence band near the first resonance in forward bias is shown in Fig. 2. The $In_{0.05}Ga_{0.95}As$ strained layer forms a prewell, adjacent to the narrow emitter barrier, into which electrons from the n^+/n contact region accumulate into 2D electron states. The onset of resonant tunneling into the GaAs QW occurs at $V_B \simeq 0.25$ V when the prewell $n=1$ subband edge (E_1) coincides with the energy of the $n=1$ conduction subband edge of the GaAs QW ($E_{1,QW}$) [see Fig. 1(a)]. The current reaches a maximum at $V_B=0.66$ V, beyond which the device switches to the off-resonant state and the current decreases abruptly. The first resonance occurs over a wide bias range since the incorporation of a relatively wide collector barrier causes space charge buildup in the GaAs QW.[2–7]

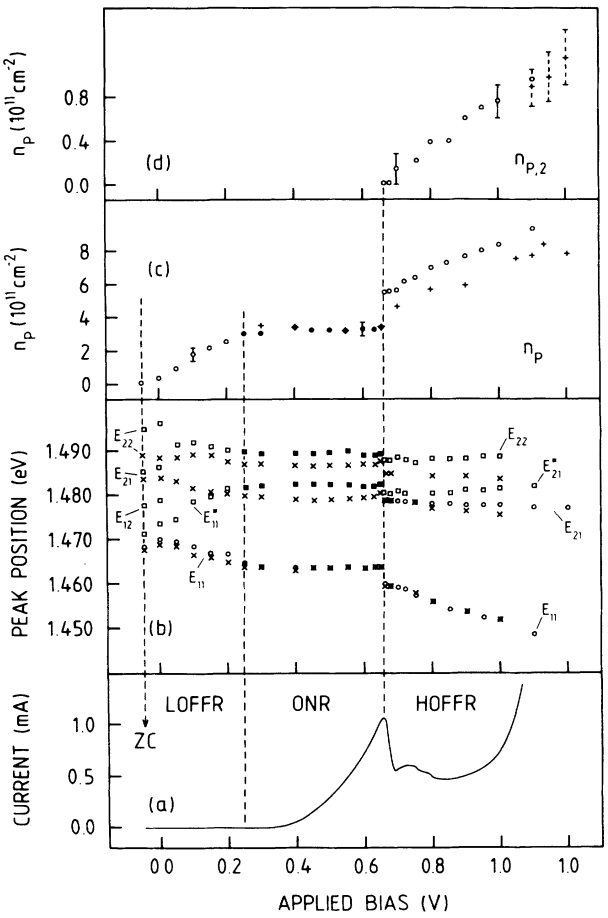

FIG. 1. (a) Current across the DBRTS, (b) PL (circles) and PLE (squares) peak positions, calculated transition energies (crosses), (c) total electron density n_p, and (d) second subband electron density $n_{p,2}$, as a function of applied bias V_B from the $In_yGa_{1-y}As$ prewell layer of the DBRTS. Open and solid symbols in (b) and (c) represent off and on resonance, respectively. For $V_B<0.66$ V the $n=1$ electron densities are determined by the Stokes shift, PL linewidth, and line shape. For $V_B>0.66$ V n_p is determined from the PL peak separation E_{21}-E_{11} and the $n=2$ Stokes shift and PL linewidth. In the off-resonant state n_p accumulates continuously whereas on-resonance n_p remains constant while charge increases in the GaAs QW. An abrupt increase in n_p is seen between the on- and off-resonance state at $V_B=0.66$ V. n_p and $n_{p,2}$ determined from magnetotransport measurements are plotted as pluses in (c) and (d); errors for $n_{p,2}$ are shown as dashes in (d).

Due to electrostatic feedback E_1 remains pinned to $E_{1,QW}$ until the quasi-Fermi level in the GaAs QW ($E_{F,QW}$) is equal to the Fermi level E_F in the prewell.[4] Beyond this bias resonant tunneling ceases and charge is expelled from the GaAs QW. The two smaller peaks in the *I-V* characteristics at 0.73 and 0.79 V are due to LO phonon-assisted tunneling.[4,24] Beyond $V_B \sim 1.0$ V the tunnel current increases strongly again due to the onset of the second resonance in which electrons tunnel in the $n=2$ electron level of the GaAs QW.

For future ease of reference in Fig. 1(a), the bias range from $V_B=0$ to 0.20 V, where the device is not yet on res-

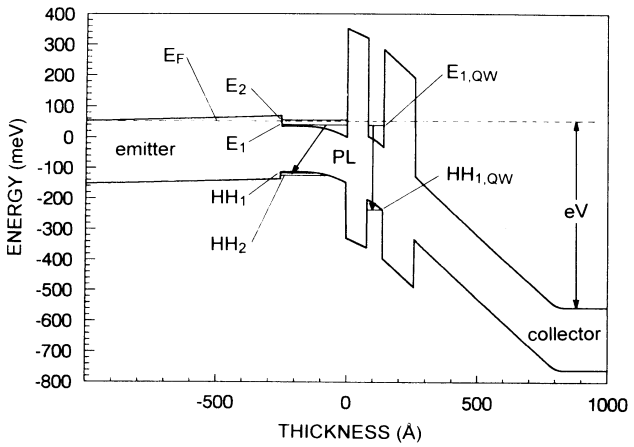

FIG. 2. Calculated diagram of conduction- and valence-band edge potential profile for the DBRTS, in applied forward bias, biased at the first resonance. Electrons tunnel from the $In_yGa_{1-y}As$ emitter prewell accumulation layer into the GaAs QW, where charge builds up as a result of the thicker collector barrier. As well as PL from the GaAs QW region, PL occurs in the emitter-accumulation region since photocreated holes are inhibited from being swept into the contact layers by the prewell barrier.

onance, is labeled LOFFR (low bias off resonance region), the region of the first resonance, $V_B=0.25$ to 0.66 V is labeled ONR (on resonance) and above $V_B=0.66$ V is labeled HOFFR (high bias off resonance).

B. Photoluminescence from the prewell

Figure 3 shows photoluminescence (PL) from the prewell as a function of bias (dashed lines), excited using below GaAs band-gap excitation of 1.484 eV. The holes are directly photocreated in the prewell and at applied biases greater than $V_B=0$ V, are inhibited from being swept into the n^+ emitter contact by the shallow prewell barrier (Fig. 2).

The photoluminescence observed up to $V_B=0.66$ V [Figs. 3(a)–3(e)] arises from recombination between electrons in the $n=1$ electron subband and holes in the first heavy-hole (HH_1) subband, and is labeled E_{11}. In the presence of free carriers PL recombination is expected to occur from electron states at wave vector $k=0$ (at the band edge) up to states corresponding to the Fermi energy ε_F with photocreated holes which thermalize to $k=0$.[25] The width of the PL spectrum will be controlled by ε_F, with a falloff in intensity towards ε_F which depends on the degree of hole localization or disorder in the system.[14,18,26]

The narrowest PL linewidth (3.2 meV) is observed at $V_B=-0.05$ V [Fig. 3(a)] since at this small reverse bias the prewell is empty of electrons. For future reference this bias is labeled ZC (zero charge). A steady increase in PL linewidth from $V_B=-0.05$ to 0.25 V (to 6.5 meV) reflects an increase in band filling of $n=1$, as the prewell charges up with increasing bias.[8] It should be noted that the charge in the prewell is not zero at $V_B=0$ V, since charge is transferred from the contacts, into the narrower gap $In_yGa_{1-y}As$ region in order to establish equilibrium at $V_B=0$ V. In these structures disorder is concluded to be small as only weak luminescence is observed at the Fermi level E_F [marked in Figs. 3(c)–3(e)]. The shoulder observed towards higher energy in Figs. 3(c)–3(e)

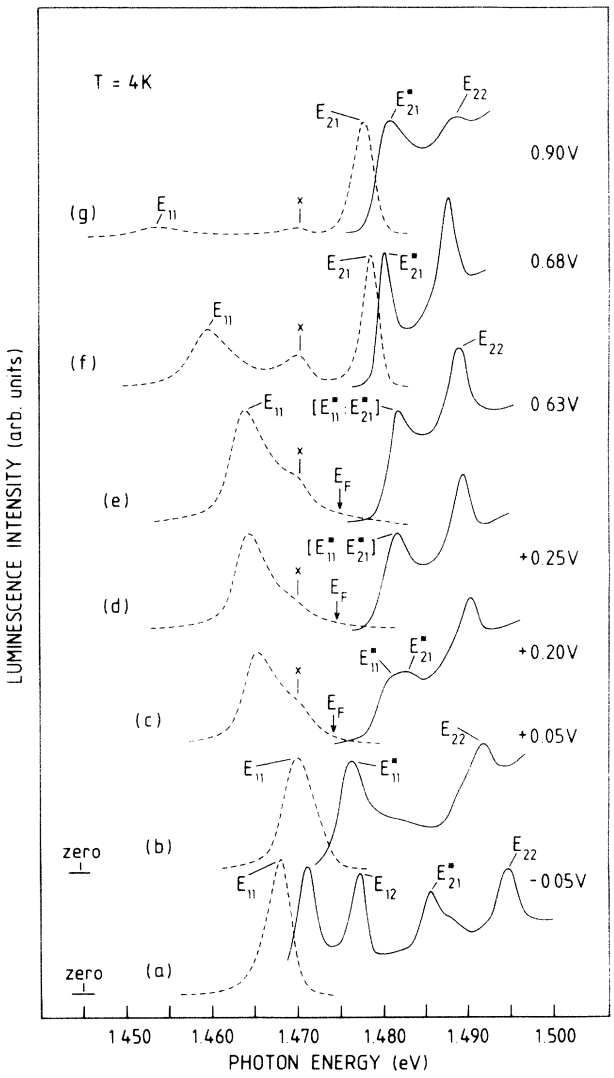

FIG. 3. PL (dashed line) and PLE (full line) at $T=4$ K from the $In_yGa_{1-y}As$ prewell layer of the DBRTS, as a function of applied bias. Increasing E_{11} PL linewidth is observed from (a) $V_B=-0.05$ V to (d) $V_B=0.25$ V, while the structure is off resonance. In the on-resonance state ($V_B\geq 0.25$ V), shown at (e) $V_B=0.63$ V, the E_{11} PL linewidth remains constant. There is an abrupt appearance of E_{21} in PL when the device switches off resonance, shown at (g) $V_B=0.68$ V and (h) $V_B=0.90$ V. At (a) $V_B=-0.05$ V four prominent peaks in the PLE (full line), E_{11}^*, E_{12}, E_{21}^*, and E_{22} are seen. The $\Delta n\neq 0$ transitions decrease in strength with increasing applied forward bias so that only E_{11}^* and E_{22} in PLE are prominent at (b) $V_B=+0.05$ V. At (c) $V_B=0.20$ V both a broad E_{11}^* and weak E_{21}^* are seen at the absorption onset and at (d) $V_B=0.25$ V and (e) $V_B=0.63$ V E_{11}^* and E_{21}^* have similar transition energies labeled $[E_{11}^*,E_{21}^*]$. In the off-resonance state, (f) $V_B=0.68$ V and (g) $V_B=0.90$ V only E_{21}^* and E_{22} are seen. At $V_B=0.90$ V the PLE transitions are broadened. The lowest intensity on the PLE spectra indicates zero intensity, except where zero is labeled.

(marked as ×) is most likely due to PL from part of the surrounding structure which is unbiased; its position is the same as the $V_B=0$ V peak position and its intensity with bias is approximately constant. The peak positions of the PL as a function of bias are plotted as circles in Fig. 1(b). Between $V_B=-0.05$ and 0.25 V the E_{11} peak position decreases by 5.5 meV.

In the ONR region, from $V_B=0.25$ to 0.66 V, the structure is on resonance and the E_{11} PL linewidth only changes a small amount [Figs. 3(d) and 3(e) at 0.25 and 0.63 V, respectively]. In addition the PL peak position remains at an approximately constant energy [Fig. 1(b)]. Both of these observations show that the quasiequilibrium charge density in the prewell remains approximately constant in the on-resonance region while charge accumulates in the GaAs QW.

The DBRTS switches into its off-resonant state at $V_B=0.66$ V [the HOFFR region in Fig. 1(a)]. At the switching bias there is an abrupt downward shift of E_{11} by 5 meV and the appearance of a second peak E_2, which arises from recombination between the $n=2$ electron level and HH_1 [Fig. 1(b)]. A comparison of the PL spectra in the on- and off-resonant states can be made at $V_B=0.63$ and 0.68 V, as shown in Figs. 3(e) and 3(f), respectively. The change in spectral form is due to an abrupt increase in the prewell electron density n_p as resonant tunneling into the GaAs QW ceases.[4,5] (The feature between E_{11} and E_{21}—marked as ×—is again attributed to the unbiased part of the sample.) Over the bias range $V_B=0.68-1.0$ V, E_{11} shifts downwards in energy by 6.8 meV with E_{21} remaining approximately constant [Fig. 1(b)]. The E_{21} linewidth increases from 2.3 to 4.0 meV between 0.68 and 1.10 V and indicates an increase in the $n=2$ electron density $n_{p,2}$ as confirmed by the PLE measurements below. Together with the increasing E_2-E_1 separation, this shows that n_p is increasing in the HOFFR region. Figures 3(f) and 3(g) show that as V_B is increased the intensity (peak height) of E_{21} relative to E_{11} increases greatly. Beyond $V_B=0.90$ V fewer holes are available for recombination in the prewell since the trapping efficiency will decrease with the higher electric field, and as a result the overall PL intensity decreases.

C. Photoluminescence excitation from the prewell

The PLE spectra measured as a function of V_B are shown by the full lines in Fig. 3 and the peak positions are plotted as squares in Fig. 1(b). The spectra are normalized to the continuum at an energy position just beyond the E_{22} exciton feature. At ZC [$V_B=-0.05$ V, Fig. 3(a)], where the narrowest linewidth is observed in PL, four prominent features are observed and are attributed to, in order of increasing energy, E_{11}, E_{12}, E_{21}, and E_{22}. (For future clarity the transitions E_{11} and E_{21} when observed as absorption peaks are labeled E_{11}^* and E_{21}^* to distinguish them from the corresponding PL recombination.) The identification of these transitions is aided by previous studies of $Al_xGa_{1-x}As/In_yGa_{1-y}As/GaAs$ modulation doped QW's (Refs. 18 and 22) and the results of simulations presented in Sec. III E. No transitions from light-hole (LH) levels are observed since strain is expected to upshift LH_1 by ~30 meV from HH_1.[27] The linewidths of E_{11}^* and E_{12} are narrow (2.9 and 1.8 meV, respectively) showing the high quality of the structure. Of particular note is that the transitions E_{12} and E_{21}^* ($\Delta n\neq 0$), normally forbidden in a symmetric square well, are of equal strength to the "allowed" transitions E_{11}^* and E_{22} ($\Delta n=0$). This indicates the presence of a significant electric field in the well.[28,29] At lower biases ($V_B<-0.05$ V) the strength of E_{12} relative to E_{11}^* increases due to a further increase in electric field.

In the LOFFR bias region (0–0.20 V), with increasing bias the strength of the $\Delta n\neq 0$ transitions initially decreases significantly. By $V_B=0.05$ V only the $\Delta n=0$ transitions E_{11}^* and E_{22} are clearly observed [Fig. 3(b)]. Beyond this bias the E_{11}^* feature broadens and weakens. In the LOFFR region E_{11}^* absorption is seen to increase in energy [plotted as squares in Fig. 1(b)] reflecting an increase in electron Fermi energy ε_F [see Figs. 3(b) and 3(c)], since absorption will only occur into unoccupied states above the Fermi level E_F.

A rather broad feature is observed at the absorption onset of the $V_B=0.20$ V PLE spectrum [Fig. 3(c)]. At $V_B=0.25$ V [Fig. 3(d)] the feature at the absorption onset has increased in strength and narrowed. We deduce that at $V_B=0.20$ V there are two partly overlapping peaks present, the weakened E_{11}^* at lower energy and E_{21}^* at higher energy. This can be understood by the following arguments. The PLE transition energy E_{11}^* is related to the Fermi energy ε_F (since ε_F is located in $n=1$) by $E_{11}^*=(1+m_e/m_h)\varepsilon_F$, where $(m_e/m_h)\varepsilon_F$ is the Moss-Burstein shift, for direct transitions, due to the presence of free carriers.[28] Therefore in the LOFFR region as V_B is increased E_{11}^* moves closer to E_{21}^*, as a result of the increasing electron accumulation. Extrapolation of the energy of E_{11}^* with increasing bias predicts E_{11}^* to be at an energy just below E_{21}^* at $V_B=0.20$ V. By similar reasoning, at $V_B=0.25$ V the transition energies E_{11}^* and E_{21}^* are estimated to be equal, as shown schematically in Fig. 4. The increase in intensity of the $[E_{11}^*:E_{21}^*]$ feature at $V_B=0.25$ V is attributed to increased E_{21}^* oscillator strength as a result of further band bending in the prewell (discussed in Sec. III E).

In the on-resonance bias region, between 0.25 and 0.65 V, the PLE spectral shape [Figs. 3(d) and 3(e)] shows very little change, consistent with the very small variation in PL linewidth observed in this bias range. When the device switches to the off-resonance state ($V_B=0.66$ V), in contrast to the PL, only a small change in the PLE spectra is observed (compare $V_B=0.63$ V [Fig. 3(e)] and $V_B=0.68$ V [Fig. 3(f)]). On increasing the bias in the HOFFR region the Stokes shift between the PL recombination E_{21} and absorption transition E_{21}^* becomes greater. This is attributed to the Moss-Burstein shift,[28] reflecting an increase in the population of $n=2$. In addition Figs. 3(d)–3(g) show that from the ONR into the HOFFR regions, towards higher bias, there is a continuing increase in the excitonic strength of E_{21}^* relative to that of E_{22}.

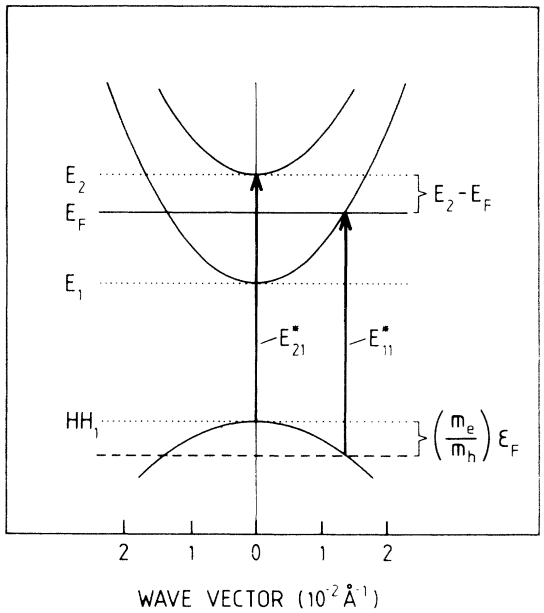

FIG. 4. Schematic dispersion curves of E_2, E_1, and HH_1 subbands showing the E_{11}^* and E_{21}^* absorption transitions at $V_B=0.25$ V. E_{11}^* and E_{21}^* transitions have the same energy because E_{21}^* occurs from $k=0$ in HH_1, whereas E_{11}^* occurs from $k=(m_e/m_h)\varepsilon_F/\hbar$. The energy difference E_2-E_F is the same as $(m_e/m_h)\varepsilon_F$.

At biases greater than 0.80 V, the $T=4$ K E_{21}^* and E_{22} excitonic transitions broaden and decrease in strength. Beyond 0.90 V the broadening is too pronounced to observe the spectral features clearly. This broadening can occur for several reasons; PLE transition linewidths do increase, as the carrier density in the subband with which they are associated with increases,[29,16] and in addition the applied electric field may bring about lifetime broadening of (especially) hole states as these are pushed towards the barrier of the shallow well.

D. Charge density in the prewell

The PL and PLE spectra will now be used to provide a measure of the charge accumulation in the emitter prewell in the bias range of interest, $V_B=-0.05$ to $+1.10$ V. From $V_B=-0.05$ V up to the start of the ONR region the most accurate way to estimate the electron density n_p is from the Stokes shift Δ_s between the peak of the E_{11} PL and E_{11}^* PLE.[28,29,22] The Fermi energy ε_F is related to Δ_s by the relationship $\Delta_s=\varepsilon_F(1+m_e/m_h)$, where m_e ($=0.07m_0$) (Ref. 30) and m_h ($=0.15m_0$) (Ref. 31) are the electron and heavy-hole masses, respectively; m_0 is the free-electron mass. At $V_B=-0.05$ V, the PL linewidth is at a minimum; therefore $n_p=0$ is assumed at this bias. A small extrinsic Stokes shift, Δ_0, at $V_B=-0.05$ of 3.0 meV is observed, due to thermalization of electrons (as well as holes) to band tail states before recombining.[32] To allow for this $\Delta_0/2$ is subtracted from Δ_s before determining ε_F. This means there is an uncertainty in Δ_s of ±1.5 meV, and hence in n_s of $\pm0.3\times10^{11}$ cm^{-2}. This method agrees well with line-shape analysis of the PL.[22] The values of n_p ($=m_e\varepsilon_F/\pi\hbar^2$) are plotted as circles in Fig. 1(c) and show n_p increases from 0 to $2.95\pm0.3\times10^{11}$ cm^{-2} from $V_B=-0.05$ to 0.20 V.

For $V_B\geq0.25$ V, in the ONR region, E_{11}^* is not distinguishable from E_{21}^*. However at $V_B=0.25$ V, we established in Sec. III C that E_{11}^* is at the same energy as E_{21}^*. The E_{11} PL spectral shape and the shift between E_{21}^* PLE and E_{11} PL do not vary significantly in the ONR region. The energy of E_{21}^* is thus taken as the lower limit for the energy of E_{11}^* in PLE. Therefore the separation of E_{21}^* PLE and E_{11}^* PL is a lower limit for the E_{11} PL to E_{11}^* PLE Stokes shift.[33] We thus conclude that n_p varies from $2.95\pm0.3\times10^{11}$ cm^{-2} to $3.4\pm0.3\times10^{11}$ cm^{-2} [Fig. 1(c), circles)] in the on-resonance region.

For $V_B\gtrsim0.66$ V, in the HOFFR region, the Fermi energy ε_F is determined from the PL peak position differences $E_{21}-E_{11}$ together with the estimated carrier density in $n=2(n_{p,2})$. $n_{p,2}$ is obtained from the Stokes shift between E_{21} in PL and E_{21}^* in PLE; a line-shape fitting analysis of $n=2$ PL also agreed well with this method.[33] From these results, it is deduced that at the switching point to the HOFFR region, there is an abrupt increase in n_p to 5.4×10^{11} cm^{-2}, beyond which n_p increases continuously to 9.3×10^{11} cm^{-2} at 1.10 V [Fig. 1(c), circles]. Correspondingly $n_{p,2}$ increases from 0 to 0.95×10^{11} cm^{-2} [Fig. 1(d), circles].

Conventional magnetotransport (I-B) measurements were also used as a separate measure of the prewell emitter density, n_p. n_p is related to the fundamental field B_F of the current magneto-oscillations by $n_p=2eB_F/h$;[34] the results are plotted as pluses in Fig. 1(c). The presence of second subband population is seen by a second slower series of oscillations superimposed on the main series and is only sensitive for $n_{p,2}\gtrsim0.8\times10^{11}$ cm^{-2}; $n_{p,2}$ is shown in Fig. 1(d) (as + with dotted error bars). The trends in the carrier densities deduced by magnetotransport are seen to agree very well with the optical measurements.

E. Comparison with calculations

In order to support an interpretation of the optical results, we performed a calculation of the emitter-band profile as a function of the emitter electron density. It is based on a self-consistent solution of Schrödinger and Poisson equations for a given electron density in the prewell, using a transfer-matrix method. In these calculations a background doping density of 10^{16} cm^{-3} was used for the emitter contact region adjacent to the prewell. No corrections for excitonic or many-body effects have been included as the calculations are primarily intended to support our identifications of the observed spectral features and to explain the trends in transition energies and oscillator strengths with bias. The calculated transition energies E_{11}, E_{21}, and E_{22} for the various electron densities are plotted at the appropriate biases as crosses in Fig. 1(b). Good agreement with the experimental transition energies is obtained. In addition, the oscillator strengths of the transitions were calculated from the square of the overlap of electron and hole wave functions.

As noted in Sec. III B, there is expected to be finite electron density in the prewell at $V_B=0$ V due to charge transfer from the contacts in order to establish equilibrium. The calculations show that at $n_p=0.3\times10^{11}$ cm^{-2} (corresponding to $V_B=0$ V in the experiment), the transition energy E_{11} is at a maximum, in agreement with the experiment. Furthermore the $\Delta n\neq0$ transitions E_{21}^* and E_{12} have very small oscillator strength, thus indicating very small average electric field in the well, associated with approximately symmetrical band bending. To fully deplete the prewell a reverse bias electric field is required, shown by the stronger oscillator strength of E_{21}^* and E_{12}, as seen experimentally at $V_B=-0.05$ V [Fig. 3(a)].

From $n_p=0.3\times10^{11}$ cm^{-2} to higher electron densities (10×10^{11} cm^{-2} calculated) the E_{11} transition energy decreases. This occurs because as more electrons accumulate in the prewell the $n=1$ electron wave function is increasingly confined in a quasitriangular potential close to the $In_yGa_{1-y}As/Al_xGa_{1-x}As$ interface while the $n=1$ holes are pushed to the opposite interface, thus leading to a reduction in transition energies.[28,18,20,32] The $n=2$ electron wave function is spread across the whole prewell, which means that with increasing bias, an increase in oscillator strength of E_{21} relative to E_{11} (f_{21}/f_{11}) is expected. The calculations predict that when $n_p=2.8\times10^{11}$ cm^{-2}, f_{21} and f_{11} are of similar strength, in good agreement with the experimental observation at $n_p=2.5\pm0.3\times10^{11}$ cm^{-2} [$V_B=0.20$ V, Fig. 3(c)]. For carrier densities greater than this f_{21} is calculated to be greater than f_{11}. This is consistent with our interpretation that the PLE peak at the absorption threshold in the ONR region has a strong E_{21} component [Fig. 3(d)].

The ratio of the E_{21} PL peak height to that of E_{11} in the HOFFR region provides an experimental estimate of the relative oscillator strength, $(f_{21}/f_{11})_{exp}$. From $n_p=6.1\times10^{11}$ cm^{-2} to 8.5×10^{11} cm^{-2} $(f_{21}/f_{11})_{expt}$ varies from 5.7 to 14.0. Taking into account a factor ~2 for excitonic enhancement of E_{21} (Refs. 15 and 18) the calculated values, 3.8–8.5, agree very well with experiment, and add further support to our interpretation of the optical spectra.

To summarize, in this section we have shown that the calculated transition-energy separations and oscillator strengths as a function of carrier density describe very well the experimentally observed optical behavior in the emitter-accumulation region.

F. Charge distribution in the asymmetric DBRTS

PL spectra from the GaAs QW region of the DBRTS (excited by a HeNe laser, energy 1.959 eV) were used to corroborate the charge distribution deduced from the prewell results. The PL spectra are very similar to that of the asymmetric DBRTS studied by Skolnick *et al.*[8,11] and are described only briefly here. The observed PL, denoted $E_{11,QW}$, arises from recombination between electrons in the $n=1$ electron subband (energy $E_{1,QW}$) and photocreated holes which tunnel into the GaAs QW from the collector contact region and thermalize to the first heavy-hole level ($HH_{1,QW}$) (see Fig. 2).

Figure 5(b) shows the variation in energy of $E_{11,QW}$

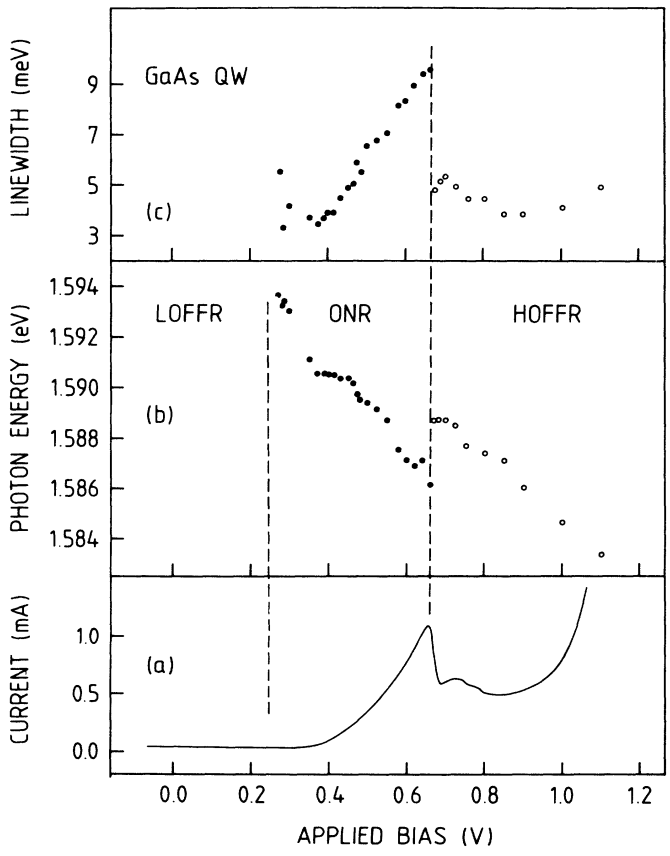

FIG. 5. (a) Current across the DBRTS, (b) $E_{11,QW}$ PL peak position, and (c) $E_{11,QW}$ PL linewidth from the GaAs QW as a function of applied forward bias V_B, in the region of the first electron resonance. Open and solid circles represent on- and off-resonance states, respectively. The decrease in the E_{11} peak energy and increase in the linewidth while the structure is on resonance (ONR region) show charge buildup in the GaAs QW.

and Fig. 5(c) shows the change in $E_{11,QW}$ linewidth as a function of V_B. The I-V characteristics are shown again in Fig. 5(a) for comparison. PL from the GaAs QW is first observed at $V_B=0.27$ V at the onset of the first resonance. In this ONR region charge accumulation in the GaAs QW is shown by the decrease in the $E_{11,QW}$ transition energy and an increase in the PL linewidth from 3.3 to 9.5 meV, consistent with charge buildup in the GaAs QW and the observation of only a very small change in the emitter prewell charge throughout this region. The maximum in $E_{11,QW}$ linewidth occurs at the peak in the I-V curve. Beyond this there is an abrupt decrease in linewidth and increase in transition energy of $E_{11,QW}$, corresponding to charge being expelled from the well; this correlates with the abrupt increase in charge observed in the emitter prewell shown in Fig. 1(c). A minimum in linewidth occurs at $V_B=0.85$ V just before the onset of the second resonance, beyond which the PL linewidth increases again. $E_{11,QW}$ also begins to redshift strongly again.

A line-shape analysis[22,8] of the PL from the GaAs QW, $E_{11,QW}$, just before the DBRTS switches off resonance gives the maximum electron density in the GaAs QW as $3(\pm 0.5)\times 10^{11}$ cm^{-2}. The optical determinations of electron density in the prewell were used to determine the maximum electron density in the GaAs QW. When the DBRTS goes off resonance all of the charge in the GaAs QW is ejected. Self-consistency is maintained by an increase in charge in the prewell of an amount almost equal to that ejected from the GaAs QW.[5] The increase in prewell electron density at the switching bias of 0.66 V is $2.1(\pm 0.6)\times 10^{11}$ cm^{-2}. From consideration of the electrostatics of the structure, using the method described in Ref. 5,[35] the maximum electron density in the well is calculated to be $2.5(\pm 0.8)\times 10^{11}$ cm^{-2}. This is in good agreement with the direct PL measurement of GaAs QW.

In summary the charging behavior of the DBRTS deduced from optical measurements of the emitter accumulation region (prewell) correlates well with direct PL measurements of the GaAs QW region.

IV. FERMI-ENERGY EDGE SINGULARITY STUDIES

The characteristic behavior of a Fermi-energy edge singularity seen in PLE is pronounced broadening and weakening of excitonlike absorption peaks with increasing temperature, up to ~ 50 K.[14–19] This characteristic is now used to study the nature of excitonic features observed in PLE from the prewell.

At ZC [$V_B=-0.05$ V, Fig. 6(a)] no significant broadening or weakening of the E_{11}^*, E_{12}, E_{21}^*, E_{22} peaks, relative to the continuum, is observed for temperatures up to 40 K. Therefore these features are all of atomic exciton nature. The absence of E_{11}^* temperature dependence is consistent with the deduction that there is a negligible density of electrons accumulated in the prewell at this bias.

In the LOFFR region, up to 0.15 V, where E_{11}^* is broader at $T=4$ K, raising the temperature to $T=20$ K gives rise to very pronounced broadening and weakening of E_{11}^* [shown at $V_B=+0.05$ V in Fig. 6(b)]. By $T=40$ K only a broad, very weak, continuum is seen. This is in marked contrast to E_{22} which is unaffected by temperature. The very strong temperature dependent behavior of E_{11}^* is characteristic of the FEES which occurs due to the significant electron density in $n=1$ in this region.[14–19]

At $V_B=+0.20$ V [Fig. 6(c)] the PLE feature at the absorption onset, at $T=4$ K, consists of a weak E_{11}^* and E_{21}^* peak of similar oscillator strength. Raising the temperature to $T=20$ K results in asymmetric broadening of this feature, attributed to the characteristic weakening of the E_{11}^* absorption peak. The slightly higher energy component is assigned to E_{21}^* which shows a much weaker temperature dependence, as expected, since the E_{21}^* excitons are of atomic exciton character, being associated with the $n=2$ subband which is not occupied[18,22] [shown by the absence of E_{21} PL in the LOFFR and ONR bias regions, Figs. 3(b)–3(e)]. Overlapping E_{11}^* and E_{21}^* peaks at 4 K are thus distinguished by the different thermal behavior of the two processes involved in creating the PLE peaks. This is illustrated more clearly at slightly higher bias, $V_B=0.25$ V, in Fig. 6(d) where the $[E_{11}^*{:}E_{21}^*]$ feature consists of E_{11}^* and E_{21}^* peaks at essentially the same energy (see Fig. 4); E_{21}^* is the dominant and probably narrower component. By contrast with the spectrum of Fig. 6(b) (dominated by an E_{11}^* FEES at the PLE onset), at $V_B=0.25$ V a pronounced PLE peak assigned to E_{21}^* excitonic transitions now clearly persists up to 40 K, while the broader underlying E_{11}^* FEES contribution to the $[E_{11}^*{:}E_{21}^*]$ feature is strongly weakened at higher temperatures. By contrast, the strength, relative to the continuum, of the prominent E_{22} feature in Fig. 6(d) remains constant. The nearly degenerate E_{11}^*,E_{21}^* excitonic processes are not expected to interact as they involve transitions between valence and conduction subband states at different energies and points in k space, as illustrated in Fig. 4. Only E_{11}^* transitions terminate at states very close to E_F. Similar temperature dependent behavior occurs to higher bias in the ONR region.

The behavior described above contrasts with that for the HOFFR region where the second subband is occupied at $T=4$ K [Figs. 3(f) and 3(g)]. As shown at $V_B=0.90$ V ($n_{p,2}\sim 0.7\times 10^{11}$ cm^{-2}) [Fig. 6(e)], raising the temperature to 20 and 40 K results in weakening and broadening of both E_{21}^* and E_{22}^*. This is characteristic behavior of a FEES associated with the $n=2$ electron subband, since both transitions involve the populated $n=2$ subband.[18,22]

To summarize, at $n_p=0$, the PLE features E_{11}^*, E_{12}, E_{21}^*, and E_{22} are of atomic exciton nature since no temperature dependent behavior up to $T=40$ K is seen. In the LOFFR region, where $n=1$ only is populated, pronounced temperature-dependent broadening and weakening of E_{11}^* is seen, indicative of a FEES associated with $n=1$. For the ONR region the combined $[E_{21}^*{:}E_{11}^*]$ peak exhibits temperature dependence even though $n=2$ is not occupied, and is attributed to the weakening of the E_{11}^* FEES component. In the HOFFR region, where $n=2$ is clearly occupied temperature dependence of both

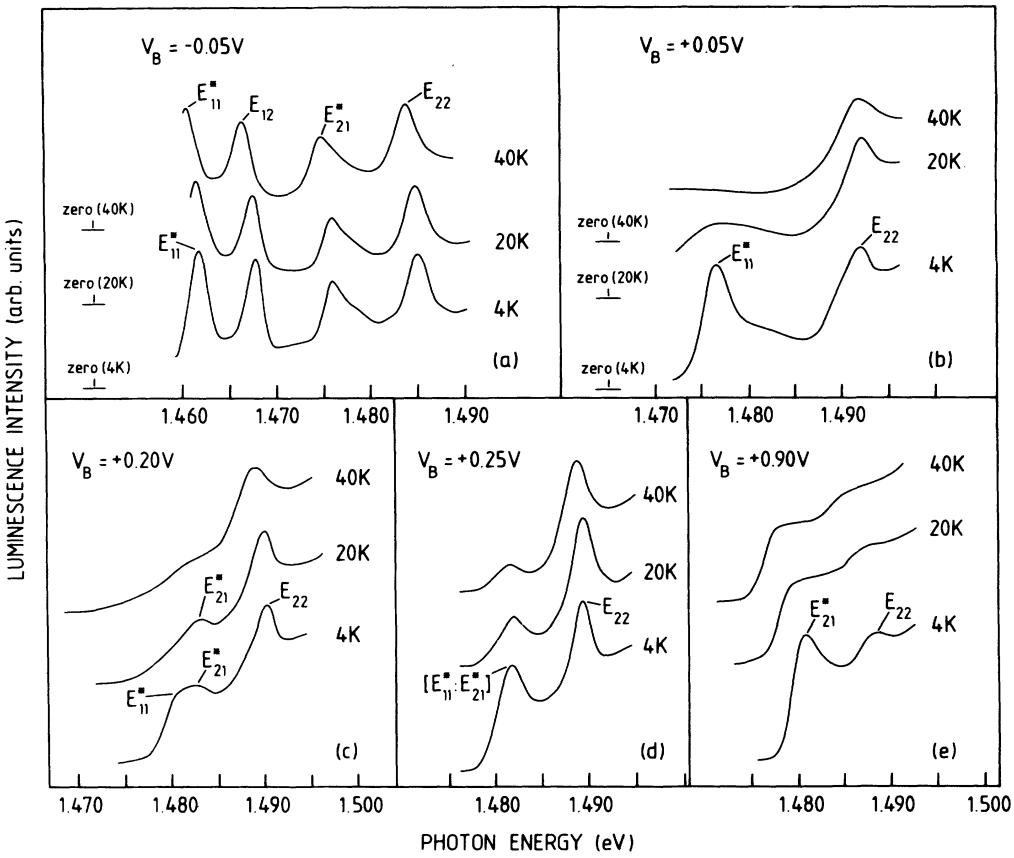

FIG. 6. PLE (full line) from the prewell of the DBRTS at $T=4$, 20, and 40 K for a range of applied biases. At (a) $V_B=-0.05$ V the PLE spectrum is unaffected by temperature indicating E_{11}^* is of atomic exciton nature. At (b) $V_B=+0.05$ V the prominent E_{11}^* feature at $T=4$ K is significantly weakened at $T=20$ and 40 K, characteristic behavior of a FEES associated with $n=1$. At (c) $V_B=0.20$ V the E_{21}^* feature is unaffected at $T=20$ K whereas the E_{11}^* FEES is weakened, giving rise to an asymmetric profile near the absorption edge. At (d) $V_B=0.25$ V, $[E_{11}^*:E_{21}^*]$ in PLE exhibits temperature dependent behavior. Since the $n=2$ subband is unpopulated this behavior is attributed to weakening of the E_{11}^* FEES. At (e) $V_B=0.90$ V E_{21} and E_{22} in PLE both show temperature-dependent behavior which is characteristic of a FEES associated with $n=2$. The lowest intensity on the spectra indicates zero intensity, except on spectra where zero is labeled.

E_{21}^* and E_{22} is seen, characteristic behavior of a FEES associated with $n=2$.

V. CONCLUSION

To summarize, the inclusion of an $In_yGa_{1-y}As$ prewell layer adjacent to the emitter barrier of a double-barrier resonant tunneling structure allows the observation of PL from the emitter-accumulation region under operation. This provides a direct measure of electron accumulation in the emitter and, by consideration of the electrostatics, a probe of the charge distribution in the whole DBRTS. The results obtained are in good agreement with direct PL measurements of the GaAs QW and with the trends in the magnetotransport measurements of the emitter. For an asymmetric DBRTS, in the off-resonance state electrons accumulate in the prewell in a continuous fashion. When the device is on resonance the charge in the prewell remains constant while charge builds up in the GaAs QW. However, charge is abruptly expelled from the GaAs QW when the DBRTS switches to the off-resonance state causing an abrupt increase in electron density in the prewell. Beyond this, charge in the prewell increases in a continuous fashion. A small reverse bias is required to deplete the prewell of equilibrium carriers; under such conditions the associated electric field is detected by observation of $\Delta n=0$ and $\Delta n\neq 0$ transitions of comparable intensity.

The tunability range of electron densities in the prewell of the DBRTS over a very wide range means that these are very suitable structures for studying the nature of excitonic features in the PLE spectra. The structures show a variation from an atomic exciton in $n=1$, to a FEES in $n=1$, through to a FEES in $n=2$.

ACKNOWLEDGMENT

We would like to acknowledge L. J. Reed for his very expert assistance in some of these measurements.

*Permanent address: Laboratoire de Microstructures et Microelectronique, Centre National de la Recherche Scientifique (L2M-CNRS), B.P. 107, 92225 Bagneux Cedex, France.

[1]L. L. Chang, L. Esaki, and R. Tsu, Appl. Phys. Lett. **24**, 593 (1974).

[2]L. Eaves, G. A. Toombs, F. W. Sheard, C. A. Payling, M. L. Leadbeater, E. S. Alves, T. J. Foster, P. E. Simmonds, M. Henini, O. H. Hughes, J. C. Portal, G. Hill, and M. A. Pate, Appl. Phys. Lett. **52**, 212 (1988).

[3]E. S. Alves, L. Eaves, M. Henini, O. H. Hughes, M. L. Leadbeater, F. W. Sheard, G. A. Toombs, G. Hill, and M. A. Pate, Electron. Lett. **24**, 1190 (1988).

[4]M. L. Leadbeater, O. H. Hughes, E. S. Alves, L. Eaves, M. Henini, G. A. Toombs, and F. W. Sheard, J. Phys. Condens. Matter **1**, 10 605 (1989).

[5]M. L. Leadbeater, E. S. Alves, L. Eaves, M. Henini, O. H. Hughes, F. W. Sheard, and G. A. Toombs, Superlatt. Microstruct. **6**, 59 (1989).

[6]A. Zaslavsky, V. J. Goldman, D. C. Tsui, and J. E. Cunningham, Appl. Phys. Lett. **53**, 1048 (1988).

[7]F. W. Sheard and G. A. Toombs, Appl. Phys. Lett. **52**, 1228 (1988).

[8]M. S. Skolnick, D. G. Hayes, P. E. Simmonds, A. W. Higgs, G. W. Smith, H. J. Hutchinson, C. R. Whitehouse, L. Eaves, M. Henini, O. H. Hughes, M. L. Leadbeater, and D. P. Halliday, Phys. Rev. B **41**, 10 754 (1990).

[9]M. Yoshimura, J. M. Schulman, and M. Sakaki, Phys. Rev. Lett. **64**, 2422 (1990).

[10]J. F. Young, B. M. Wood, G. C. Aers, R. L. Devine, M. C. Liu, D. Landheer, M. Buchanan, A. J. Springthorpe, and P. Mandeville, Phys. Rev. Lett. **60**, 2085 (1988).

[11]M. S. Skolnick, P. E. Simmonds, D. G. Hayes, A. W. Higgs, L. Eaves, O. H. Hughes, G. W. Smith, A.D. Pitt, C. R. Whitehouse, M. J. Hutchinson, C. R. H. White, and M. Henini, Phys. Rev. B **42**, 3069 (1990).

[12]W. I. E. Tagg, M. S. Skolnick, M. T. Emeny, A. Higgs, and C. R. Whitehouse, Phys. Rev. B **46**, 1501 (1992).

[13]M. Riechert, D. Bernklau, J. P. Reithmaier, and R. D. Schnell, Electron. Lett. **26**, 340 (1990).

[14]M. S. Skolnick, J. M. Rorison, K. J. Nash, D. J. Mowbray, P. R. Tapster, S. J. Bass, and A. D. Pitt, Phys. Rev. Lett. **58**, 2130 (1987).

[15]G. Livescu, D. A. B. Miller, D. S. Chemla, M. Ramaswamy, T. Y. Chang, N. Sauer, A. C. Gossard, and J. H. English, IEEE J. Quantum Electron. **QE-24**, 1677 (1988).

[16]M. K. Saker, M. S. Skolnick, P. A. Claxton, J. S. Roberts, and M. J. Kane, Semicond. Sci. Technol. **3**, 691 (1988).

[17]S. R. Andrews, A. S. Plaut, R. T. Harley, and T. M. Kerr, Phys. Rev. B **41**, 5040 (1990).

[18]M. S. Skolnick, D. M. Whittaker, P. E. Simmonds, T. A. Fisher, M. K. Saker, J. M. Rorison, R. S. Smith, P. B. Kirby, and C. R. H. White, Phys. Rev. B **43**, 7354 (1991).

[19]A. E. Ruckenstein, S. Schmitt-Rink, and R. C. Miller, Phys. Rev. Lett. **56**, 504 (1986); S. Schmitt-Rink, C. Ell, and H. Haug, Phys. Rev. B **33**, 1183 (1986); A. E. Ruckenstein, S. Schmitt-Rink, and R. C. Miller, Phys. Rev. Lett. **53**, 504 (1986); J. Gavoret, P. Nozieres, B. Roulet, and M. Combescot, J. Phys. (Paris) **30**, 987 (1989).

[20]W.Chen, M. Fritze, A. V. Nurmikko, D. Ackley, C. Colvard, and M. Lee, Phys. Rev. Lett. **64**, 2434 (1990); W. Chen, M. Fritze, A. V. Nurmikko, M. Hong, and L. L. Chang, Phys. Rev. B **43**, 14 738 (1991); W. Chen, M. Fritze, W. Walecki, A. V. Nurmikko, D. Ackley, J. M. Hong, and L. L. Chang, *ibid.* **45**, 8464 (1992).

[21]P. Hawrylak, Phys. Rev. B **44**, 3821 (1991); **44**, 6262 (1991).

[22]T. A. Fisher, P. E. Simmonds, M. S. Skolnick, A. D. Martin, and R. S. Smith, Phys. Rev. B **48**, 14 253 (1993).

[23]N. G. Anderson, W. D. Laidig, R. M. Kolbas, and Y. C. Lo, J. Appl. Phys. **60**, 2361 (1986).

[24]V. J. Goldman, D. C. Tsui, and J. E. Cunningham, Phys. Rev. B **36**, 7635 (1987); M. L. Leadbeater, L. Eaves, E. S. Alves, M. Henini, O. H. Hughes, A. Celeste, J. C. Portal, G. C. Hill, and M. A. Pate, *ibid.* **39**, 3483 (1989).

[25]M. S. Skolnick, K. J. Nash, M. K. Saker, S. J. Bass, P. A. Claxton, and J. S. Roberts, Appl. Phys. Lett. **50**, 1885 (1987).

[26]S. K. Lyo and E. D. Jones, Phys. Rev. B **38**, 4113 (1988).

[27]G. Ji, D. Huang, U. K. Reddy, T. S. Henderson, R. Houdré, and M. Morkoc, J. Appl. Phys. **62**, 3366 (1987).

[28]See, for example, C. Delalande, G. Bastard, J. Orgonasi, J. A. Brum, H. W. Liu, M. Voos, G. Weimann, and W. Schlapp, Phys. Rev. Lett. **59**, 2690 (1987).

[29]H. Yoshimura, G. E. W. Bauer, and M. Sakaki, Phys. Rev. B **38**, 10 791 (1988).

[30]D. F. Nelson, R. C. Miller, and D. A. Kleinman, Phys. Rev. B **35**, 7770 (1987); R. People and S. K. Sputz, *ibid.* **41**, 8431 (1990).

[31]E. D. Jones, H. Ackerman, J. E. Schirber, and T. J. Drummond, Solid State Commun. **55**, 525 (1985); G. C. Osbourn, J. Vac. Sci. Technol. A **3**, 826 (1985).

[32]M. H. Meynadier, J. Orgonasi, C. Delalande, J. A. Brum, G. Bastard, M. Voos, G. Weimann, and W. Schlapp, Phys. Rev. B **34**, 2482 (1986).

[33]In the ONR region, PL alone cannot be used to estimate n_p since the position of E_F in PL is not clearly seen.

[34]Further details on magnetotransport determination of carrier density in DBRTS's can be found in Refs. 3–5.

[35]The extra charge in the prewell (2.1×10^{11} cm^{-2}) in the off-resonance state at $V_B=0.66$ V is smaller than the charge in the GaAs QW (2.5×10^{11} cm^{-2}) in the on-resonance state at 0.66 V, since the field due to charge in the GaAs QW acts over a smaller distance. For a given applied bias extra charge is needed in the GaAs QW than in the prewell, because the same charge density as in the prewell would give rise to a smaller voltage drop in the structure. Further details of the electrostatic considerations can be found in Refs. 4 and 5.